EDUZONE: International Peer Reviewed/Refereed Multidisciplinary Journal (EIPRMJ), ISSN: 2319-5045
Volume 5, Issue 2, July-December, 2016, Impact Factor: 3.842, Available online at: www.eduzonejournal.com

Effect of Temperature on the Coordination Chemistry of Cu (II)-Trimethoprim Complexes as Studied by Density Functional Theory

Dr. Ashish Garg

Department of Chemistry, Seth R. N. Ruia Govt. College, Ramgarh Shekhawati, Sikar, Rajasthan, India

ABSTRACT

Density Functional Theory (DFT) was used for the computational study of two empirically produced copper trimethoprim complexes with distinctly different geometries. Crystallographic information was used to determine the initial geometries of copper-trimethoprim complexes 1, 2, and 3. Using B3LYP/BLYP hybrid density functional methods with 6-31G and LANL2DZ basis sets at 298 and 352 K, the geometries of complexes 1, 2, and 3 were fully optimized. After comparing the obtained results with the actual data, it was determined that complex 1 is the most stable geometry, whereas complex 3 is an unstable/intermediate geometry that can be transformed into a stable form through recrystallization. In addition, when comparing LANL2DZ with 6-31G, the latter foundation set provides more precise results (in terms of experimental validity).

Keywords: Coordinated chemistry; density functional theory (dft) approach; copper; trimethoprim; metallic complexes

INTRODUCTION

Synthetic antibacterial antibiotic and member of the diaminopyrimidine (pyridine-3,4-diamine) family, also known as trimethoprim (2,4-diamino-5-(3,4,5-trimethoxybenzyl)pyrimidine, TMP). Trimethoprim works by inhibiting the enzyme dihydrofolate reductase (DHFR). In the presence of NADPH, this enzyme catalyzes the conversion of 7,8-dihydrofolate to 5,6,7,8-tetrahydrofolate. The antibiotic trimethoprim blocks the conversion of dihydrofolic acid to tetrahydrofolic acid in bacteria [1, 2] (Figure 1).

In the treatment of pneumocystis pneumonia infections in AIDS patients, it is often used with sulfamethoxazole because it is effective against the most prevalent bacterial species.

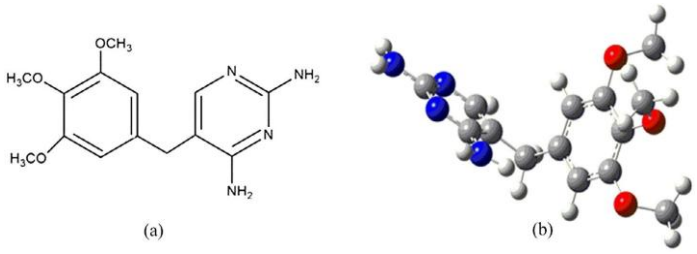

Figure 1. (a) 2d structure of trimethoprim; (b) 3d structure of trimethoprim.

Humans [3], bacterial infections (both Gram-positive and -negative) [4]. However, for the prevention and treatment of simple UTIs, trimethoprim alone is sufficient [5].

Among the ligands that comprise a pyrimidine ring system, trimethoprim is a well-known biological agent. The pyrimidine ring system is included in a large number of therapeutically relevant chemicals. Several vitamins, coenzymes, and antibiotics found in nucleic acids possess a pyrimidine ring that can serve as a binding site for metal ions. The use of substituted 2,4-diaminopyrimidine compounds as metabolic inhibitors of protein and nucleic acid production pathways [6] is widespread.

Trimethoprim complexes and Schiff bases have also been studied for their potential applications in coordination chemistry. For example, 1, 10-phenanthroline has a greater bacteriostatic effect than the ligand on rumen bacteria [7], acid-fast bacteria [8], and many gram-positive bacteria [9] when present in body fluids or tissue cells, even on those that have high resistance to antibiotic itself. It has been discovered that the bacteriostatic effects of metal complexes of

sulfa-drugs are greater than those of the medicines themselves [10, 11]. Trimethoprim interacts with metal ions as a monodentate ligand while having seven potential binding sites for metal ions (e.g., trimethoprim complexes with metal (II/III)).

III), including copper (II), zinc(II), platinum(II), rhodium(II), cadmium(III), cobalt(III), and cobalt(II).

The coordination chemistry of trimethoprim organometallic complexes is crucial. Antibacterial and antimicrobial activity is enhanced, and it forms stable complexes with most transition metals. Square planar, tetrahedral and octahedral geometries are formed by the complexes of trimethoprim with transition metal ions [6, 12–14]. For example, when ethanolic solutions of trimethoprim and copper acetate monohydrate were mixed and refluxed for two hours [12] (Figures 2 and 3), olive-green crystals of Cu(II)-trimethoprim complexes (complexes 1 and 2) with distorted octahedral geometry were formed. By combining ethanolic solutions of trimethoprim with copper acetate monohydrate at 20-25 °C [15] (Figure 4), a light-blue Cu(II)-trimethoprim complex (complex 3) with a distorted square planar shape was produced.

Copper-trimethoprim complexes of two distinct sorts were produced at two temperatures from the same concentration of reactants. The complex generated between 20 and 25 °C (complex 3) [15] involves the linking of three copper atoms with distinct oxidation states. In

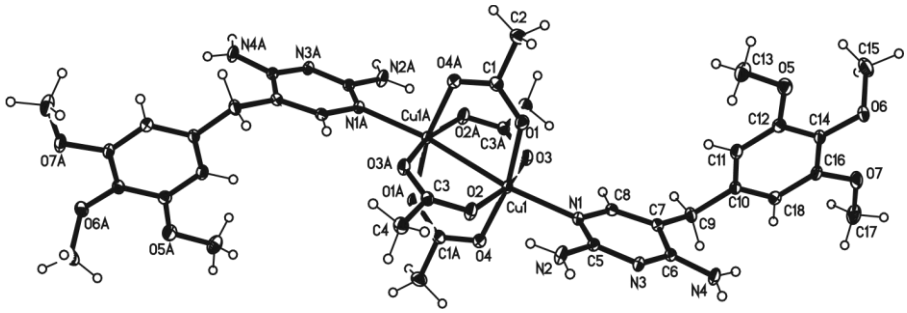

Figure 2. Crystal structure of copper trimethoprim complex **1** at 75–80 ° C

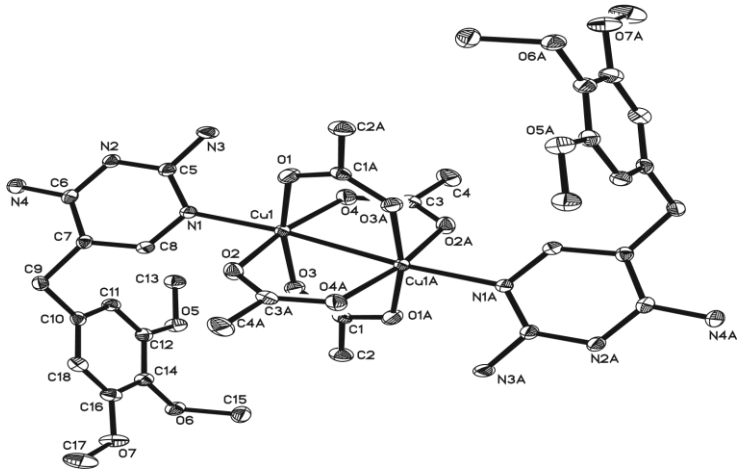

Figure 3. Crystal structure of copper trimethoprim complex **2** at 75–80 °C

In complex 3, the metal (Cu) centers each display deformed tetrahedral geometry as well as oxidation states of both +1 and +2.

A filthy olive-green amorphous Cu-TMP complex was produced when ethanolic solutions of copper acetate monohydrate and trimethoprim were combined at boiling temperature and refluxed for two hours. The amorphous phase, which is a dirty olive greencolor, crystallizes into two isomeric geometrical forms of olive green crystals (complex one and complex 2), both of which exhibit Cu-Cu linkage in which each Cu atom exhibits +2 oxidation states [12].

The goal of this research is to use density functional theory (DFT) to characterize the coordination chemistry of Cu (II)-trimethoprim complexes with a variety of geometrical structures at a range of temperatures [12, 15]. Calculated molecular geometries and optimization energies were compared to experimental data using density functional theory.

Research is being conducted on the electrical and structural features of the complexes in their ground states in both the gas and solvent phases.

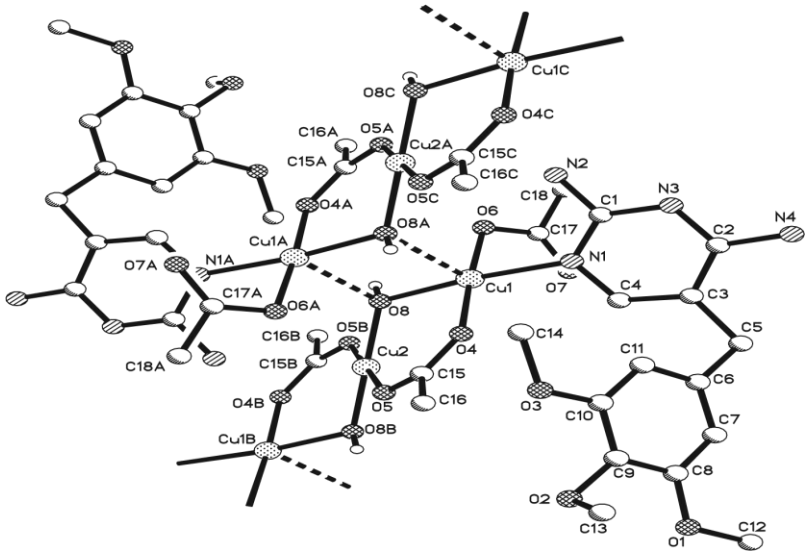

Figure 4. Crystal structure of copper trimethoprim complex **3** at 20–25 °C

Mathematical Specifics

The crystal structures of complexes 1, 2, and 3 (CCDC Nos. 619488 and 619490) have been improved using the hybrid density functional theory (DFT) methods Gaussian G09 [16] with B3LYP and BLYP [17, 18]. The research makes use of the basis sets 6-31G and LANL2DZ. Geometry optimizations were performed at temperatures of 298 and 352 K. Single-point energy calculations were performed in both the gas and solvent phases using B3LYP and BLYP hybrid density functions. The effective core potential basis set of Stuttgart-Dresden (SDD) was used to determine single-point energies for all atoms except Cu and H (= 0.600 for C, 1.154 for O, and 0.864 for N). We used the conductor-like polarizable continuum method (CPCM) [20] to perform SCRF (self-consistency reaction field) computations [19] on optimal geometries in water and ethanol as solvents.

DISCUSSION AND RESULTS

Urinary tract infections (UTIs) that are not particularly difficult can be treated with trimethoprim (TMP) alone as an antibiotic. It's effective against both Gram-positive and Gram-negative aerobic bacteria, and it's absorbed orally to be dispersed throughout the body's fluids and tissues [21]. Co-trimoxazole, which combines trimethoprim and sulfamethoxazole, has been in use for quite some time.

Trimethoprim metal complexes were repeatedly synthesized in the lab. In the presence of Pd(II) and Pt(II), trimethoprim produces square planar complexes [14]. Low-spin octahedral complexes of trimethoprim have been observed with Mn(II), Co(II), Ni(II), Fe(II), and Zn(II) [13]. Trimethoprim with Zn (II) formed a tetrahedral complex [6]. There is a high activity constant value [22] in Cu(II) trimethoprim complexes.

Additionally, Schiff base complexes of Zn(II) and Cu(II) with trimethoprim and sulfamethoxazole were produced [23].

But among metals, Cu(II) has been investigated the most. Copper has been shown to have positive effects in treating a variety of disorders, including gastric ulcers, rheumatoid arthritis, and cancer. In addition, it transports oxygen [12].

This paper presents a DFT investigation into the (a) coordination chemistry of trimethoprim complexes 1, 2, and 3 and (b) synthesis of trimethoprim complexes with copper acetate as reported in the literature. Two distinct (olive-green) geometrical complexes are produced at 352 K, according to the literature.

Changing the temperature alone led to the formation of geometric complexes with varying amounts of atoms and hues. At 298 K, a distorted square planar complex (light-blue colored) is created, involving three copper atoms, and these complexes obtained also exhibit various antibacterial activity. The acetate and hydroxide bridges between these three copper atoms are very strong.

This is accomplished by doing DFT calculations utilizing a total of four different basis sets (6-31G, LANL2DZ, and hybrids B3LYP and BLYP). Validity was achieved by comparing computational results generated using two distinct DFT methods and basis sets with one another and with experimental data.

Copper-Trimethoprim Complicated Geometry Optimization

Gas-phase B3LYP/LANL2DZ, B3LYP/6-31G, BLYP/LANL2DZ, and BLYP/6-31G DFT optimizations (Figures 5-8) were performed on the copper acetate, trimethoprim, and copper-trimethoprim complexes (1, 2, and 3). Formation energies of copper-trimethoprim complexes were computed (Tables 1-3). Tables 4-9 also display the structural properties of the optimized and computed geometries.

Intricate 1

As can be seen in Table 1, the relative energies of complex one computed at 298 and 354 K using B3LYP/LANL2DZ, B3LYP/6-31G, BLYP/LANL2DZ, and BLYP/6-31G levels of hybrid DFT are all quite similar, ranging from 19.9 to 21.1 kcal/mol. Based on the data, we know that the maximum relative energy of 19.9 kcal/mol was achieved by

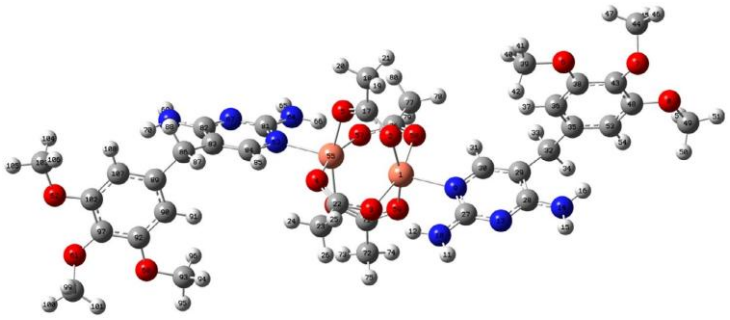

Figure 5. optimized geometry of complex **1**.

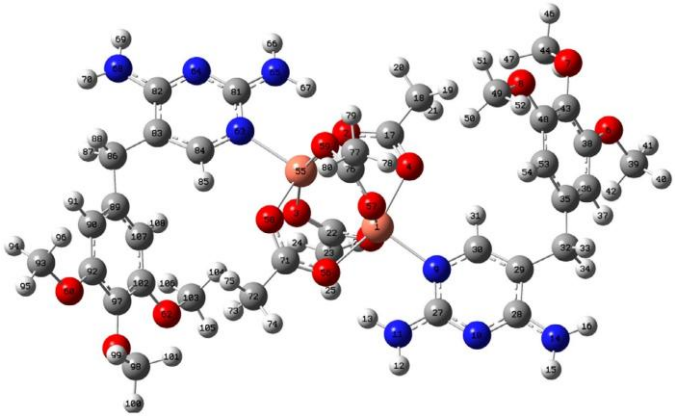

Figure 6. optimized geometry of complex **2**.

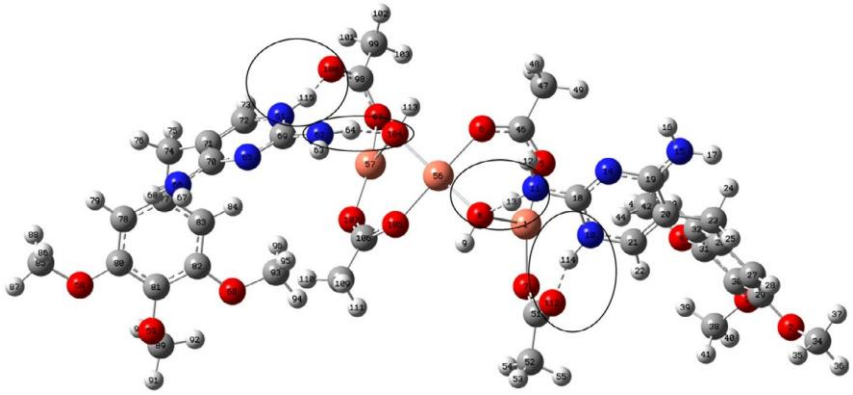

Figure 7. disrupted optimized geometry of complex **3** at lanl2dZ basis set.

BLYP/6-31G at both 298 and 352 K, while B3LYP/LANL2DZ at both temperatures yielded the lowest allowable energy of 21.1 kcal/mol. As can be shown in Tables 1, 4, and 5 and Figure 5, the average bond lengths of the predicted and experimental copper-trimethoprim complexes are very close, with a difference of 0.1.

Intricate 2

The relative energies computed for complex two at 298 and 352 K using the same hybrid density functional theory levels as used for complex one varied significantly, with a 9.9 kcal/mol (7.4 to 17.3 kcal/mol) difference.

The minimum relative energy for complex one is given by LANL2DZ (Table 1).

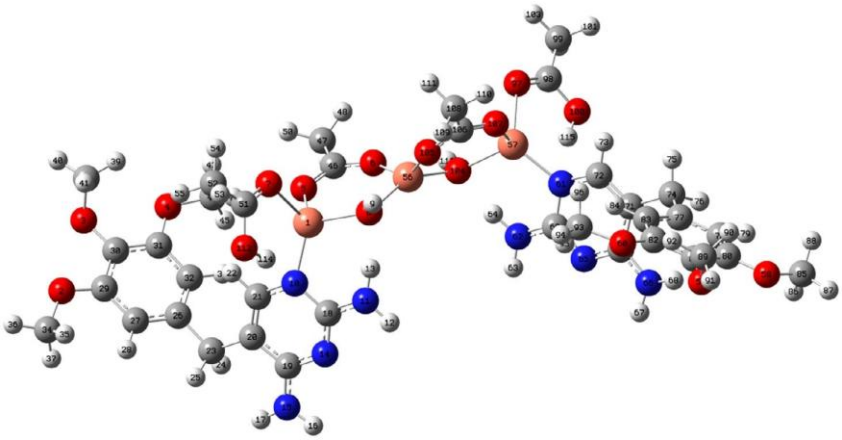

Figure 8. optimized geometry of complex **3** at 6-31G basis set.

Table 1 Complex 1's Relative Energy Values (In Kcal/Mol)

	Complex **1**							
	298 K				352 K			
	B3LYP		BLYP		B3LYP		BLYP	
	6-31G	LANL2DZ	6-31G	LANL2DZ	6-31G	LANL2DZ	6-31G	LANL2DZ
opt.	−11.85	−12.79	−10.40	−12.84	−11.83	−12.79	−10.40	−12.35
sdd	−12.80	−12.87	−11.59	−14.21	−12.78	−12.89	−11.59	−12.72
CPCm-Water	−21.44	−21.24	−20.20	−22.05	−21.44	−21.13	−20.20	−24.11
CPCm-ethanol	−21.15	−20.95	−19.90	−21.77	−21.14	−20.84	−19.90	−20.08

Table 2. relative energy values (kcal/mol) of complex **2**.

	Complex **2**							
	298 K				352 K			
	B3LYP		BLYP		B3LYP		BLYP	
	6-31G	LANL2DZ	6-31G	LANL2DZ	6-31G	LANL2DZ	6-31G	LANL2DZ
opt.	−7.41	−7.98	−5.58	−6.06	−7.38	−7.98	−5.59	−6.06
sdd	−7.38	−7.79	−4.60	−0.57	−7.37	−7.81	−4.61	−6.40
CPCm-Water	−16.39	−17.67	−14.60	−9.07	−16.38	−17.55	−14.60	−20.04
CPCm-ethanol	−16.06	−17.31	−14.24	−8.76	−16.05	−17.2	−14.24	−15.91

Table 3. relative energy values (kcal/mol) of complex **3**.

	Complex **3**							
	298 K				352 K			
	B3LYP		BLYP		B3LYP		BLYP	
Jobs	6-31G	LANL2DZ	6-31G	LANL2DZ	6-31G	LANL2DZ	6-31G	LANL2DZ
opt.	81.22	29.56	52.09	19.53	81.23	28.72	52.09	19.53
sdd	76.87	47.28	64.97	33.16	76.86	47.28	61.67	34.65
CPCm-Water	68.69	41.56	56.92	25.21	68.71	41.56	52.18	23.15
CPCm-ethanol	69.03	41.81	57.25	25.54	69.04	41.81	52.57	27.23

Bond lengths (Å)	Complex **1** at 352 K					Complex **1** at 298 K			
	Exp.	B3LY-P/6-31G	BLY-P/6-31G	B3LYP/ LANL2DZ	BLYP/ LANL2DZ	B3LY-P/6-31G	BLY-P/6-31G	B3LYP/ LANL2DZ	BLYP/ LANL2DZ
Cu1–Cu55	2.7052	2.7048	2.8214	2.8715	2.8861	2.7999	2.8214	2.8717	2.886
Cu1–o1	1.9846	1.9788	2.0051	2.0426	2.0491	1.9764	2.0051	2.0426	2.049
Cu1–o3	1.9666	2.0227	2.0227	2.0207	2.0736	2.0251	2.0227	2.0209	2.0736
Cu1–o58	1.9792	2.0137	2.0166	2.0446	2.0705	2.016	2.0166	2.0444	2.0705
Cu1–o59	1.9846	1.9739	2.0051	2.0223	2.0498	1.9718	2.005	2.0224	2.0498
Cu1–n9	2.2079	2.1616	2.1872	2.1901	2.2084	2.1608	2.1872	2.19	2.2084

Table 5. Bond angles of Cu-methoprim complex **1**.

Bond angles (°)	Exp.	Complex **1** at 298 K				Complex **1** at 352 K			
		B3LYP/ 6-31G	BLYP/ 6-31G	B3LYP/ LANL2DZ	BLYP/ 6-31G	B3LYP/ LANL2DZ	BLYP/ 31G	B3LYP/ LANL2DZ	BLYP/ 6-LANL2DZ
o(2)–Cu(1)–Cu(55)	79.71	82.57	83.16	81.79	82.06	79.61	82.35	82.35	82.01
C(17)–o(2)–Cu(1)	128.55	124.74	124.46	125.46	124.83	122.57	123.89	124.43	124.69
n(9)–Cu(1)–Cu(55)	172.75	178.13	178.13	177.63	177.79	179.27	179.47	177.63	177.36

Table 6. Bond lengths of Cu-methoprim complex **2**.

Bond lengths (Å)	Complex **2** at 352 K					Complex **2** at 298 K			
	Exp.	B3LYP/ 6-31G	BLYP/ 6-31G	B3LYP/ LANL2DZ	BLYP/ LANL2DZ	B3LYP/ 6-31G	BLYP/ 6-31G	B3LYP/ LANL2DZ	BLYP/ LANL2DZ
Cu1–Cu55	2.7052	2.8012	2.7983	2.8427	2.89	2.8012	2.7979	2.8426	2.89
Cu1–o1	1.9846	1.9555	2.0242	2.0484	2.0497	2.0529	2.0109	2.0483	2.0497
Cu1–o3	1.9666	1.9514	1.9979	2.0062	2.0779	1.9557	2.0237	2.0063	2.0779
Cu1–o58	1.9792	2.042	2.0075	2.063	2.0623	2.0415	2.0099	2.0079	2.0623
Cu1–o59	1.9846	2.0535	2.0365	2.0079	2.0499	1.9516	2.0119	2.0609	2.0499
Cu1–n9	2.2079	2.1552	2.1799	2.1758	2.2087	2.1719	2.1794	2.1758	2.2087

Table 7. d angles rimethop omplex **2**.

Bond angles (°)	Exp.	Complex **2** at 298 K				Complex **2** at 352 K			
		33LYP/ 6-31G	BLYP/ LANL2DZ	B3LYP/ 6-31G	BLYP/	B3LYP/ 6-31G	LANL2DZ	BLYP/ LANL2DZ	B3LYP/ LANL2DZ	BLYP/ 6-31G
o(4)–Cu(1)–Cu(55)	79.7	82.6	83.2	81.8	82.1	79.6	82.4	80.3	82.0	
C(17)–o(4)–Cu(1)	128.6	124.7	124.5	125.5	124.8	122.6	123.9	124.2	124.7	
n(9)–Cu(1)–Cu(55)	172.8	178.1	178.1	177.6	177.8	179.3	179.5	177.4	177.4	

Bond lengths (Å)	Complex **3** at 298 K					Complex **3** at 352 K			
	Exp.	B3LYP/ 6-31G	BLYP/ 6-31G	B3LYP/ LANL2DZ	BLYP/ LANL2DZ	B3LYP/ 6-31G	BLYP/ LANL2DZ	B3LYP/ 6-31G	BLYP/ LANL2DZ
Cu1–n(10)	2.0228	1.93407	1.93584	3.41813	3.4442	1.9341	1.93548	3.4181	3.4436
Cu1–o8	1.9416	2.03838	2.01749	2.24771	2.1180	2.0384	2.01479	2.2475	2.1180
Cu1–o5	1.9496	2.02091	2.01754	1.94411	1.9615	2.0209	2.01754	1.9441	1.9615
Cu1–o7	1.9518	2.14419	2.11748	1.93110	1.9457	1.1442	2.11748	1.9311	1.9457
Cu56–o6	1.9544	1.95843	1.97732	1.99978	2.1032	1.9584	1.97732	1.9997	2.1033
Cu56–o8	1.9110	1.91100	1.94273	1.93237	1.9859	1.9256	1.94273	1.9323	1.9860

Table 9. rimethop omplex **3**.

Bond angles (°)	Exp.	Complex **3** at 298 K				Complex **3** at 352 K			
		B3LYP/ LANL2DZ	BLYP/ LANL2DZ	B3LYP/ 6-31G	BLYP/	B3LYP/ 6-31G	6-31G	BLYP/ LANL2DZ	B3LYP/ LANL2DZ	BLYP/ 6-31G
o(8)–Cu(1)–o(5)	90.21	106.79	109.12	58.91	104.32	106.79	109.12	97.43	104.32	
o(5)–Cu(1)–o(7)	177.11	100.23	98.38	155.58	151.03	100.23	98.37	159.85	151.03	
o(8)–Cu(1)–n(10)	174.35	113.75	113.00	75.65	78.92	113.75	113.00	75.66	78.93	
o(5)–Cu(1)–n(10)	86.71	111.69	109.32	91.90	92.49	111.68	109.32	91.91	92.43	
Cu(1)–o(8)–Cu(56)	122.2	118.48	116.59	100.7	109.86	118.48	116.59	100.70	109.84	
C(46)–o(5)–Cu(1)	136.41	126.97	126.63	128.86	127.79	126.97	126.63	128.86	127.78	
C(18)–o(2)–Cu(1)	180	19.87	19.92	25.86	26.11	19.87	19.92	25.86	26.11	

Intricate 3

The experimentally observed structure of complex 3 is drastically different from that predicted by the computational study. When optimizing with the LANL2DZ basis set, the N (10) of trimethoprim forms a bond with the acetate oxygen (112) via the hydrogen (114), while the N(11) of trimethoprim attaches with the hydroxyl oxygen (8) via the hydrogen (13), breaking the trimethoprim bond with copper. The attachment pattern shown at one trimethoprim molecule is also seen at the other trimethoprim molecule (Figures 7 and 8).

It has been calculated that complex 3 possesses intermediate geometry but not product geometry. The relative energies of complex 3 are significantly greater than those of complexes 1 and 2, ranging from 19.5 to 81.2 kcal/mol, and the geometry of complex 3 distorts/breaks down during optimization at the B3LYP/LANL2DZ and BLYP/LANL2DZ levels of DFT. Complex three is hypothesized to have an unstable geometry in comparison to Complexes 1 and 2, and as such, may constitute a transition state between Complexes 1 and 2 that can be achieved through refluxing the complex solution. There is a discrepancy of 0.78 between the calculated and experimental bond lengths in copper-trimethoprim complex three (Tables 3, 8, and 9).

Using B3LYP/BLYP hybrid DFT with 6-31G/LANL2DZ as basis sets, we find that the optimization energies for complex 2 are much higher than those for complex one across the board. Based on the numbers in Tables 1 and 2, it appears that the production of the more sophisticated of the two was prioritized. The computational result demonstrates that, in comparison to other geometries, complex 1 is the most stable and dominant structure. The larger formation of complex one was experimentally confirmed as well.

It is expected that a single stable geometry can be established by repeating the crystallization process after comparing the geometry optimization of complexes 1 and 2.

Assessment of the Different Hybrid Density Functional Approaches

Computational analysis comparing hybrid density functional methods has shown that for complex one geometry, the BLYP hybrid DFT method yields lower relative energies by 0.1 kcal/mol compared to the results obtained using the B3LYP DFT method. The BLYP hybrid DFT approach yields 0.1 kcal/mol less energy compared to the B3LYP hybrid DFT method for other geometries (complex two and complex 3).

Sets of Assumptions Compared

When analyzing transition metal complexes computationally, it has been found that the LANL2DZ basis set provides more accurate (closer to experimental) results than 6-31G. Results obtained at 298 and 352 K show the same pattern, i.e., B3LYP/LANL2DZ delivers more acceptable results than B3LYP/6-31G, and similarly, BLYP/LANL2DZ produces more acceptable results than BLYP/631G.

Temperature's Impact

As was previously mentioned, both 298 and 352 K were used to optimize all of the geometries. Energy levels calculated using the hybrid DFT methods B3LYP/LANL2DZ, B3LYP/6-31G, BLYP/LANL2DZ, and BLYP/6-31G are all found to be quite close to one another. At both temperatures, the observed difference in results is less than 5 kcal/mol. Hence the results are not statistically different.

Solvent's Influence

The optimized geometries of complexes 1, 2, and 3 were subjected to SCRF (Self-consistent reaction field) simulations with the default solvent, water, and ethanol as a solvent in Gaussian-09 using a conductor-like polarizable continuum model (CPCM). The relative energies calculated using B3LYP/6-31G for complex 1 are lower than those calculated using the same method for complex 2 in the default (21.44 kcal/mol), water (21.44 kcal/mol), and ethanol (21.15 kcal/mol) solvents. Similarly, the relative energies calculated using B3LYP/LANL2DZ are smaller for complex 1 (21.13, 21.13, and 20.84 kcal/mol) than they are for complex 2 (17.55, 17.55, and 17.2 kcal/mol). Using the BLYP hybrid density functional technique has shown the same results as using the B3LYP method.

Compared to complexes 1 and 2, complex three at 298 K has greater relative energy values under all the aforementioned conditions, as shown by CPCM data. Relative energies calculated using B3LYP/LANL2DZ are lower than those calculated using B3LYP/6-31G, which are 68.69 kcal/mol for default solvent, 68.69 kcal/mol for water, and 69.03 kcal/mol for ethanol as solvent, respectively. Similarly, the relative energy values in solvent are smaller for BLYP/LANL2DZ than they are for BLYP/6-31G (25.21 kcal/mol vs. 56.92, 56.92, and 57.25 kcal/mol in the default solvent, water, and ethanol, respectively).

Changing the solvent from ethanol to water does not significantly alter the relative energy values obtained from the computational analysis of complexes 1, 2, and 3 in SCRF using CPCM as the default solvent and CPCM as the ethanol solvent. It is also noted that complex 1 has lower relative energy values at all conditions. As a result, we expect more of the former because it is more stable than the latter. The amount of one created at 352 K was likewise found to be more than the amount of two by experimental means. Higher relative energy estimates for complex three at 298 K indicate

that this is not the product but rather an intermediate shape. Computational results suggest that a single stable shape can be obtained by increasing the temperature and repeating the recrystallization process twice or three times.

CONCLUSION

The B3LYP/BLYP techniques and 6-31G/LANL2DZ basis sets were used in DFT calculations of the 1, 2, and 3 geometry copper-trimethoprim complexes. When we compared the experimental findings with the computer analyses, we discovered a good agreement. There was no appreciable difference between the energy values measured at 298 K and 352 K, despite the fact that all geometries were properly optimized at both temperatures. As a result, we conclude that temperature does not play a substantial role. When compared to complex 2, complex 1 has the lowest energy value and is the more stable geometry. Furthermore, experimental data have shown that a more complex creation occurs. The recrystallization process can transform the unstable geometry of complex three into a stable one, as indicated by the significantly higher energy value of this complex. It was determined that the order of stability is 1 > 2 > 3.

Computational outcomes additionally demonstrate that B3LYP/LANL2DZ and BLYP/LANL2DZ generate more trustworthy/comparable outcomes than B3LYP/6-31G and BLYP/6-31G, respectively.

REFERENCES

[1]. S.Bhattacharya, A.S.P. Ray. Pharmacology, Elsevier, 2, 406, (2009).
[2]. E.P. Quinlivan, J. McPartlin, D.G. Weir. FASEB J., 14, 2519 (2000).
[3]. L . Huang, A. Cattamanchi, J.L. Davis, S.D. Boon, J. Kovacs, S. Meshnick, R.F. Miller, P.D. Walzer, W.
[4]. Worodria, H. Masur. Proc. Am. Thoracic Soc. ATS J., 8, 294 (2011).
[5]. A.V.M. Franco. Best Practice Res. Clin. Obst. Gyn., 19, 861 (2005).
[6]. M. Mashkovskii. Drugs [in Russian], Vol. 1, pp. 275, Novaya Volna, Moscow (2000).
[7]. N. Demirezen, D. Tarınc, D. Polat, M. Cesme. Spectrochim. Acta, Part A, 129, 52 (2014).
[8]. W .W. Brandt, F.P. Dwyer, E.D. Gyarfas. Chem. Rev., 54, 959 (1954).
[9]. I. Georgieva, N. Trendafilova. J. Phys. Chem. A, 111, 13075 (2007).
[10]. L. Chen, T. Liu, C. Ma. J. Phys. Chem. A, 114, 443 (2009).
[11]. Y . Niu, S. Feng, R. Qu, Y. Ding, D. Wang. Int. J. Quantum Chem., 111, 991 (2011).
[12]. S.I. Gorelsky, L. Basumallick, J. Vura-Weis, R. Sarangi, K.O. Hodgson, B. Hedman, K. Fujisawa, E.I. Solomon. Inorg. Chem., 44, 4947 (2005).
[13]. U. Habib, A. Badshah, U. Flörke, R.A. Qureshi, B. Mirza, N. Islam, A. Khan. J. Chem. Cryst., 39, 730 (2009).
[14]. A. Aderoju, S.M.W. Osowole, K. Alao Olaoluwa. World Appl. Sci. J., 33, 336 (2015).
[15]. P.A. Ajibade, O.G. Idemudia. Bioinorg. Chem. Appl., 2013, 8 p. Article ID: 549549 (2013). doi:10.1155/2013/549549.
[16]. U. Habib, A. Badshah, U. Flörke, R.A. Qureshi, B. Mirza, N. Nazar-ul-Islam, A. Khan. J. Chem. Crystallogr., 39, 607 (2009).
[17]. M.J. Frisch, G.W. Trucks, H.B. Schlegel, G.E. Scuseria, M.A. Robb, J.R. Cheeseman, G. Scalmani, V. Barone, B. Mennucci, G.A. Petersson. Gaussian09, Gaussian Inc., Rev. A.2, Wallingford, CT (2009).
[18]. A.D. Becke. Phys. Rev. A, 38, 3098 (1988).
[19]. Lee, W. Yang, R.G. Parr. Phys. Rev. B, 37, 785 (1988).
[20]. Marten, K. Kim, C. Cortis, R.A. Friesner, R.B. Murphy, M.N. Ringnalda, D. Sitkoff, B. Honig. J. Phys. Chem., 100, 11775 (1996).
[21]. M.D. Liptak, G.C. Shields. J. Am. Chem. Soc., 123, 7314 (2001).
[22]. R.N. Brogden, A.A. Carmine, R.C. Heel, T.M. Speight, G.S. Avery. Drugs, 23, 405 (1982).
[23]. A.C. Tella, J.A. Obaleye. Int. J. Chem. Sci., 8, 1675 (2010).